Heritage Science

RESEARCH

Open Access

Possible modifications of parchment during ion beam analysis

Ákos Csepregi[1,2], Zita Szikszai[1*], Piotr Targowski[3], Marcin Sylwestrzak[3], Katharina Müller[4], Róbert Huszánk[1], Anikó Angyal[1], Boglárka Dönczö[1], Zsófia Kertész[1], Máté Szarka[1] and Ina Reiche[5,6]

Abstract

Ion beam analysis (IBA) is an established method to determine the concentration and the distribution of elements in art and archaeological objects. However, especially for organic specimens, caution must be taken to avoid harmful effects. In this work, the possible modification of recent calf parchment samples by proton beam irradiation was investigated applying fluences (given as deposited charge per unit area) both within and beyond the usual analytical practice. Attenuated Total Reflection Fourier Transform Infra-red Spectroscopy (FTIR-ATR) and Optical Coherence Tomography (OCT) were employed to assess changes, inspected from the surface of the samples. Although both techniques are apt to detect alterations of parchment in general, in the case of particles, which deposit the majority of their energy below the surface these techniques could not detect changes at low fluences. However, a simple "bath test" (short immersion in liquid) proved that disintegration within the material had already happened. After the "bath test", OCT and digital 3D microscopy were used to check the discontinuities in the material, especially for low fluences when the visual inspection might have missed them. Unfortunately, simply monitoring organic objects such as parchment during or after ion beam irradiation, non-destructively, is not sufficient to claim absolute harmlessness, as some studies in the past did. In line with our former findings using electron microscopy on cross sections, we found that 2.3 MeV protons with a deposited charge of 0.5 μC/cm^2 caused no changes affecting the integrity of parchment but 2 μC/cm^2 apparently did under the applied experimental conditions. To ensure the required analytical signal at a relatively low deposited charge, the detection system must be optimized for efficiency. Nevertheless, since the variability of the historic materials and the measurement set-ups are considerable, these values cannot be taken as absolutes, but only as guides, both for further IBA studies and for studies conducted in the past.

Keywords: Ion beam analysis, Proton irradiation, PIXE, Parchment, Collagen, Organic materials, Fourier transform infra-red spectroscopy in attenuated total reflectance (FTIR-ATR), Optical coherence tomography (OCT), Digital 3D microscopy, IPERION

Introduction

During the past decades, a lot of efforts have concentrated on the scientific study of cultural heritage materials to expand our knowledge concerning the chemical and physical properties of art objects. Regardless of being immovable or movable, the aim is to uncover or clarify their contextual background, and to safeguard their durability and accessibility by future generations. To this purpose, the uniqueness of heritage artefacts demands analytical methods and technologies that do not cause any damage to their integrity [1]. As a result, non-invasive techniques have experienced a large development over the past years as regards their application in heritage science [2]. However, certain analytical techniques, which are perceived in principle as non-invasive, given that their application requires no sampling, may actually cause some visible or non-visible, reversible or

*Correspondence: szikszai.zita@atomki.hu

[1] Institute for Nuclear Research (ATOMKI), Bem tér 18/C, 4026 Debrecen, Hungary
Full list of author information is available at the end of the article

irreversible changes depending on the type of material examined and the experimental parameters [3–7].

Since these problems arise for all intense radiation sources (accelerators, synchrotrons, lasers, gamma irradiation facilities, etc.) a common approach to monitor, understand and mitigate radiation-induced alterations was proposed in collaboration with IAEA and also taken up by the IPERION CH (Integrated Platform for the European Research Infrastructure ON Cultural Heritage) and IPERION HS (Integrated Platforms for the European Research Infrastructure ON Heritage Science) EU H2020 projects. Some of the results from these collaborations can be found in IPERION JRA papers [1, 8–14]. Dialogue with curators, conservators and other concerned professionals has also been initiated.

Ion beam analysis (IBA) is well-established in the field of heritage science encompassing the study of both cultural and natural heritage [15, 16]. It is often described as non-invasive and non-destructive, since no sampling is needed for most of the applications, and the measured material is preserved, but this "safe" aspect has its limits. Colour changes have been observed affecting the appearance of the object or even reflecting weakening of the structure of the material that may cause further disintegration. Nevertheless, these changes have been mostly observed in non-heritage context where they did not cause special grievance. Some of the changes are obvious immediately after the experiment, some may remain hidden but manifest themselves later on through further deterioration of the sample. Although there exist numerous studies concerning ion beam effects on various materials [17], the literature focused on heritage materials is far from being extensive [3].

With all the shared issues concerning alterations induced by other types of irradiations, some of the aspects may be more specific to ion beam analysis, for example, assessing changes below the surface layer, which might not be observable with the commonly used surface techniques. Better understanding how artefacts—especially the ones containing organic matrices, such as parchment—interact with ion beams have crucial importance for the benefit of heritage science.

Parchment has been used since Antiquity as writing and drawing support. Ancient manuscripts, which have been preserved until today, are unique testimonies to the life of people in earlier times. Parchment is made from the dermis of animal skin, such as calf, goat and sheep. It has a complex physical and chemical nature and is considered sensitive to environmental changes or microbiological attack. The analysis must preferably be non-destructive and non-invasive or, where appropriate, based on micro-sampling. The main constituent of parchment is collagen, but it also contains significant amount of water (10–15%) [18–20]. Collagen in skin is arranged in a hierarchical structure. Collagen fibres are composed of fibrils, which are made up of collagen molecules. The collagen molecule itself is composed of individual peptide chains. In skin, the collagen fibres are mainly arranged in a two-dimensional felt-like network which provide both a certain degree of flexibility and strong resistance [21]. On the molecular level, collagen is a trimeric protein formed by association of three polypeptide chains. The three strands are supercoiled around each other forming a triple helix. A ladder of backbone N–H···O=C hydrogen bonds links adjacent strands. In addition to this interstrand hydrogen bonding, hydrogen bonds are also formed through a water molecule (HB-network water) between two peptide groups on different strands. Water molecules also surround the triple helix, and act as cushion or spacer. In general, different groups of water molecules are present, from strongly bound to relatively free molecules [22].

Several micro-destructive or non-invasive methods can be used to analyse parchment such as the micro hot table method [23], NMR and thermal microscopy [24] or polarised light microscopy [25].

Organic heritage materials are less frequently analysed by IBA than metals, glass, ceramics or minerals, nevertheless studies, mostly applying Proton Induced X-ray Emission (PIXE), have been conducted [26–30], which raises the question of trade-off between the analytical signal (i.e. detection limits for the concentration of elements) and safety. In a previous work, we have characterized irradiated parchment samples using imaging methods on cross-sections [31]. Here, we focus on a non-invasive analytical approach to preserve the integrity of the sample and thereby avoid a possible influence of sample preparation on the results. The aim of this study was to monitor modifications of the samples caused by the irradiation during IBA as a function of the applied conditions and to assess, if possible, 'safe boundaries' for IBA in this model case.

Attenuated Total Reflection Fourier Transform Infrared Spectroscopy (ATR-FTIR) and Optical Coherence Tomography (OCT) complemented with digital 3D microscopy were employed semi-quantitatively to characterize alterations of parchment collagen and, thus, to help better comprehend the systemic effect of ion beam irradiation on complex organic matrices such as parchment. The results obtained by PIXE during irradiation of the samples can be exploited to probe the analytical performance of the method in relation with the collected charge (fluence). A "bath test" (immersion in liquid) was also introduced as a post-irradiation treatment to assess the weakening of the irradiated material in a simple way.

This work aims to draw attention to occasional undesirable degrading effects of applied non-destructive analysis methods and to show the applicability and limitations of potential monitoring methods.

Materials and methods

Parchment samples

The samples originate from fresh parchment prepared from calfskin. In order to thin it down and to smoothen its surface, first scraping with a glass shard, then polishing with abrasive paper (grit size 600) and squeezing with an agate stone had occurred. The parchment had a relatively heterogeneous thickness of 150–370 µm. Pieces of approximately 2×2 cm^2 were cut [31].

Irradiation

The irradiations were conducted using the external microprobe installed at the 5 MeV Van de Graaff accelerator of the Institute for Nuclear Research (ATOMKI), Debrecen, Hungary [32]. A focused proton beam (100 microns) was extracted through a thin Si_3N_4 window from the vacuum chamber and scanned over the area (approx. 0.1 cm^2). The energy of the protons was 2.3 MeV at contact with the parchment samples. The applied currents were 250 pA, 500 pA, and 1 nA while the collected charges were 25, 50, 100, 200, 300, 400, 500 and 1000 nC on a spot of approx. 3.1 mm × 3.1 mm, corresponding to deposited charge in the range of 0.25–10 µC/cm^2.

Each irradiated spot was compared to the same, but non-irradiated area on the given piece of parchment. Each piece of parchment contained 3–4 irradiated spots.

Additional irradiation was performed in the vacuum chamber of the same set-up, under approx. 10^{-6} mbar pressure.

Post-irradiation treatment ("bath test")

Selected samples were treated with a short (5-min-long) immersion either in distilled water or in a 3% hydrogen-peroxide (H_2O_2) solution at room temperature. This is a fast, non-standard test allowing the easy investigation of the resistance and the integrity of the material after irradiation as it enhances the observed effects of irradiation. Thus, it enables us to highlight changes in a first approximation. We refer to this immersion as "bath test". The H_2O_2 solution was also applied specifically on the discolorations, using a cotton bud, to check the effect of an oxidizing agent on the discoloration.

Applied analytical methods

Particle induced X-ray emission

Particle induced X-ray emission (PIXE) analysis was performed using a silicon drift X-ray detector (SDD) with ultra-thin Si_3N_4 window (manufactured by RaySpec, 30 mm^2 active area, 129 eV FWHM resolution at 5.9 keV). The detector was mounted with a permanent magnet (1 T magnetic field) which protected the detector from scattered protons. The obtained PIXE spectra were evaluated with the GUPIXWIN program code [33].

Infra-red spectroscopy in attenuated total reflection mode

Fourier Transform Infra-red Spectroscopy in Attenuated Total Reflectance (FTIR-ATR) mode is a common technique for the identification of a wide range of inorganic and organic materials. It is based on the interaction of infra-red radiation with matter. Molecules absorb at frequencies that are characteristic for their composition and structure. The obtained FTIR spectrum is showing a certain number of absorption bands, each corresponding to a specific chemical bound and vibrational mode.

The infra-red spectroscopic measurements were carried out subsequent to the irradiations with a diamond head Bruker Alpha type Attenuated Total Reflectance Fourier Transform Infra-red Spectrometer equipped with DLaTGS detector (4 cm^{-1} resolution, 24 scans recorded per each spectrum). Equal force was applied to all samples during the measurements. The analysing depth was around ~1.66 µm (at 1000 cm^{-1}). Data were collected and analysed using Opus 7.5 software. For samples that were also subjected to the bath test, the bath test was applied after the FTIR-ATR measurements.

Optical coherence tomography

Optical Coherence Tomography (OCT) is a technique for depth-resolved non-invasive imaging of weakly scattering objects. It originates from ophthalmology and has been successfully used there as a diagnostic tool since the 1990s [34]. By using near infra-red light to unravel the internal structure of examined objects, OCT permits localization of all the discontinuities and other rapid changes of the refractive index of the tested medium.

Optical Coherence Tomography is based on a concept of low-coherence interferometry. A narrow beam of light is scanned over the object. The depth of penetration is determined by absorption properties of the medium examined. By parallel transfer of the penetration beam to consecutive, adjacent positions, the whole image of the cross-section (B-scan) is built up. By repeating of such images in parallel, adjacent planes volume data is collected. The technique finds many applications in heritage science [35–37] especially for imaging sub-surface structure of paintings [38] but also historic glass [39] and other materials. Since the technique is fast and may be used on-site it was also used for monitoring of conservation treatments [40]. It was also applied for examination of parchment [41, 42], but so far only to a limited extent.

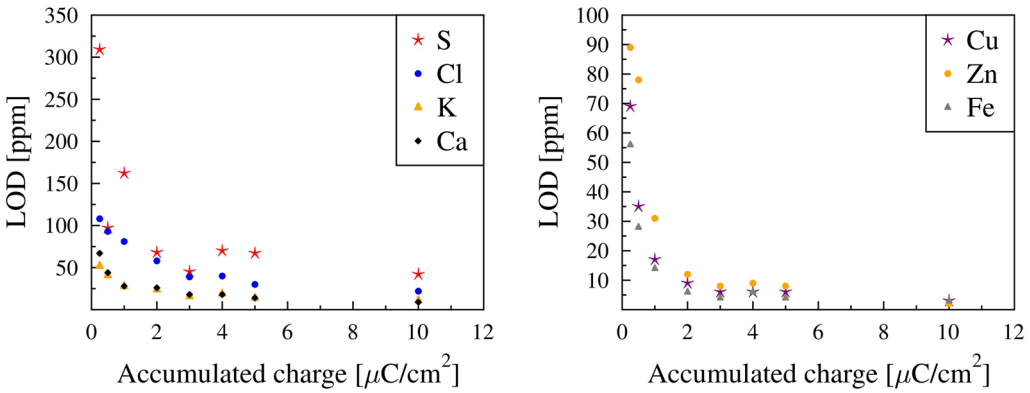

Fig. 1 PIXE detection limits for the applied X-ray detector optimized for lighter elements. Beam spot size: 0.1 cm^2

The results (B-scans) are usually presented as cross-sectional views. In this contribution in a false colour scale, where areas from which no signal is detected (perfectly transparent or beyond the range of penetration) remain black. Areas which weakly scatter or reflect the probing beam are shown in colours from blue to green, while those highly scattering or reflecting are represented by warm colours (from yellow to red). In OCT tomograms usually the vertical scale is elongated for better readability and to reflect the difference in axial (higher) and lateral (lower) resolution. In principle, OCT as an optical probing technique, delivers all vertical distances as optical ones and thus elongated within the medium by its refraction index. All tomograms presented herein are corrected for this effect with the common refractive index $n_R = 1.45$ which value was matched numerically for the best correction effects. It is worthwhile to note that possible local discrepancies from this common value would result in the imaging differences below the resolution of the tomogram.

The examination has been made with a prototype high resolution portable SdOCT instrument built under EU FP7 CHARISMA Programme. Major technical parameters of the instrument: spectral range of the probing light: 770–970 nm, axial resolution: 3.3 µm in air and 2.3 µm in the material, axial imaging range: 1.4 mm, lateral resolution: 12 µm, power of probing light at object: no more than 1 mW, distance to the object: 43 mm. More details about the construction and data processing can be found in [36].

All OCT tomograms are expanded vertically four-fold for better readability covering an area of 7 mm × 0.7 mm; scale bars represent 200 µm in both directions. In case of the samples subjected to immersion in liquid ("bath test"), OCT was performed after they had dried.

Digital 3D microscopy

High resolution images were recorded by a Keyence VHX-6000 digital 3D microscope. Single 20–200 zoom lens was used at different magnifications with reflective illumination.

Results and discussion

PIXE detection limits as a function of the collected charge

PIXE showed the presence of Si, P, S, Cl, K, Ca, Ti, Fe and Zn, as minor and trace level constituents of the parchment samples. Si, P, S, Cl, K, Ca, Fe and Zn are present in skin tissue in general, additional amount of some of these (e.g. Si, S, Ca) and the appearance of titanium might be due to the making process. Silicon (4000 ppm) could only be detected with the highest accumulated charge (10 µC/cm^2, i.e. 1 µC on the irradiated spot), while phosphorus (300 ppm) appeared at 1 µC/cm^2, i.e. 100 nC on the irradiated spot. Sulphur (2000 ppm), chlorine (600 ppm), potassium (140 ppm), and calcium (2800 ppm) could be seen even at 0.25 µC/cm^2, i.e. 25 nC on the irradiated spot while titanium (30 ppm), iron (60 ppm) and zinc (20 ppm) could be easily identified from 1 µC/cm^2 charge density, i.e. 100 nC on the irradiated spot. Figure 1 shows the detection limits as a function of the accumulated charge for the applied detector and measurement parameters. For most of the elements, a marked decrease could be seen from 0.25 µC/cm^2 to 2 µC/cm^2, then no further considerable decrease was depicted. We note that the detection limits are related to the number of incoming particles, that is to the actual collected charge, while the possible modifications are related to the fluence (charge per area). The size of the irradiated spot was always the same, 0.1 cm^2, therefore we indicated the collected charge as deposited on a unit area on the x-axis of Fig. 1, as well as consistently at the other parts of this paper. We also note that the PIXE detector was an SDD

detector with 200 nm silicon–nitride window and with a 4 cm long magnet in front of it to protect the detector from scattered protons hitting it, that is, a detector with small solid angle, optimized for lighter elements. When only heavier elements are of interest (such as metals in ink or paint on the parchment), detectors of far more efficiency can be used, and applying detector clusters is also possible [43], thus lower detection limits can be reached.

Discolouration occurring in the parchment

After irradiation, a yellowish colour was observed which faded rapidly for the lower doses, within minutes, and more slowly for the higher doses. The colour disappeared when the sample was kept under ambient temperature, pressure and humidity. Storage in dark or light conditions made no observable differences. However, a 3% H_2O_2 solution bleached it instantly. To test the role of oxygen, we irradiated a few test pieces in vacuum and kept the samples in the vacuum chamber, in this case the yellow colour was still there even after 3 days but disappeared when the samples were exposed to the atmospheric conditions. For the applied collected charges (0.25–10 μC/cm^2) the colour change (visible from the surface) was mostly reversible and could have been easily missed for the lower doses. The reversibility and the role of oxygen may point towards the formation of free radicals which were neutralized subsequently, similarly to reversible colour formation in polymers [44]. Nevertheless, deep in the material irreversible colour changes also occurred, as it was seen in cross sections [31], possibly caused by double bond formations and the extended conjugation systems. For the highest dose, the yellow colour was found to be permanently visible even from the surface, without sectioning.

Infra-red spectroscopy

For collagen the most relevant bands are the amide I, II, III, A and B bands. Amide I corresponds to the C=O stretching vibration with some contribution from CN stretching. Amide II mainly related to NH bending and CN stretching, while amide III is a complex band of several modes. Amide A is risen from NH stretching vibration and amide B is coming from a Fermi resonance between the first overtone of amide II and NH stretching [45, 46].

In this study, we focus on the amide I and II bands, which are the most extensively discussed bands in the heritage science context (Fig. 2). Table 1 summarizes the positions (local maxima) and relative intensities obtained for the non-irradiated areas in six samples. Peak areas were calculated with simple integration of absorbance values, between 1480 and 1580 cm^{-1} for amide II, and between 1580 and 1700 cm^{-1} for amide I. We found

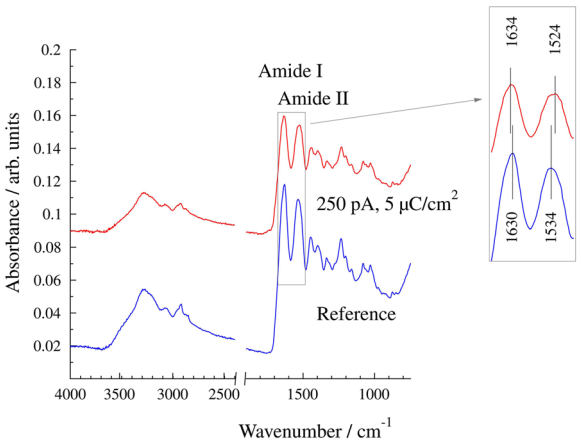

Fig. 2 FTIR-ATR spectra of a sample irradiated with 2.3 MeV protons, applying 250 pA current until the accumulated charge reached 5 μC/cm^2 (red), as well as of a reference, i.e. non-irradiated area on the same piece of parchment (blue)

Table 1 Location of amide I and amide II bands and amide I/amide II peak area ratio in the FTIR spectra of reference areas of the parchment pieces

n = 6	Position of amide I (cm^{-1})	Position of amide II (cm^{-1})	Distance (cm^{-1})	Amide I/Amide II peak area ratio
Mean ± SD	1632 ± 3	1538 ± 3	95 ± 2	1.063 ± 0.007

the maximum of the amide I band around 1632 cm^{-1}, similarly to Sendrea [47] (1631 cm^{-1}), Boyatzis [48] (1629 cm^{-1}), or Derrick [49] (1629–1635 cm^{-1}). The maximum of the amide II band was at around 1538 cm^{-1}, also in accordance with literature data (Sendrea [47] 1540 cm^{-1}, Boyatzis [48] 1542 cm^{-1}, Derrick [49] 1540–1544 cm^{-1}). The variability of the distance of the two main amide peaks did not exceed the reproducibility of the device (4 cm^{-1}), while the peak area ratios differed by less than 2%. More detailed data alongside the corresponding data for the irradiated spots are available in Additional file 1: Table S1.

The three main natural degradation paths for collagen are denaturation, hydrolysis and oxidation, which are all irreversible [50]. Denaturation occurs when hydrogen bonds holding together the collagen molecule secondary structure are broken due to some effects such as addition of heat or water, or radiation. The weakening of the hydrogen bonds can be monitored in the FTIR spectrum through the shift of the amide II peak to lower wave numbers, thus increasing the separation of the two main characteristic peaks for collagen [49, 51, 52]. On the other hand, the amide I peak might shift to higher wave numbers since it corresponds to stretching vibration, while

amide II is mostly a bending vibration, and it is a general characteristic of stretching and bending vibrations that hydrogen bonds decrease and increase their frequencies, respectively [53].

Figure 3 shows the change in the amide I–amide II distance relative to the reference value. The corresponding numerical data are available in Table S1. The FTIR-ATR spectra showed an increase of the distance of the amide I and amide II absorbance peaks for the 5 and 10 μC/cm^2 collected charges at all three currents, and also for the 3–4 μC/cm^2 in case of the lowest (250 pA) current. The amide II peak shifted from 1534–1540 cm^{-1} down to 1522 cm^{-1} at most, from a higher wave number associated with a more ordered structure to a lower one corresponding to a more disordered state. These findings are similar to that of Cappa et al. [23] who investigated the effects of mixed light-thermal ageing on parchment or to that of Vyskočilová [54] who applied a xenon lamp to leather, another collagen-based material.

According to Derrick, hydrolysis can be observed in the FTIR spectra through the amide I/amide II peak ratio. The idea is that an increase is caused by the OH^- vibrational band, originating from water molecules, overlapping with the amide I region. Derrick hypothesizes that this is bound water [49]. Mallamace et al., who studied lysozyme protein, found that bulk water which overlaps with amide I consists of the non-HB-network water molecules, i.e. those that do not directly participate in hydrogen bonding between peptide groups, while the HB-network water peak is situated between the amide I and II peaks [20]. Kudo et al. studied the adsorption of water to collagen, although the region around amide A is discussed in more detail in relation with the peak areas of different water contributions, free and bound [55]. In our case, the amide I/amide II peak area ratio increased by approx. 5% in the case of the highest collected charge (10 μC/cm^2), while there is an indication of increase (2–3%) in the 2–5 μC/cm^2 region, especially for the lowest current condition. However, in our case the change in the ratio is caused rather by the relative decrease in amide II than by the increase of amide I. First, in case of archaeological parchments or in experimental studies hydrolysis is associated by a marked increase in the amide I/amide II ratio, in our case we found only a small one, similar to the xenon lamp irradiation study mentioned above on leather [54] (Fig. 4, the corresponding numerical data are available in Additional file1: Table S1). In case of FTIR spectrometry, the absolute intensities of absorbance peaks can only be considered with caution as the experimental condition affects these values greatly, so the relative intensities are used most of the time. Nevertheless, as we took reference measurements only a few millimetres away from the irradiated spots and only a few minutes apart in time, and used the same pressure, we most probably can consider the absolute values, too, not withholding the variability inherent in the measurements. Doing so, we can state that we could not see any indication for the growth of the amide I peak. However, apparently the contribution of the amide II peak tends to be somewhat smaller for the irradiated samples than for the non-irradiated ones. This phenomenon could be caused by the structural scission of the amide group, or by the loss of the triple helical or secondary structure of the collagen

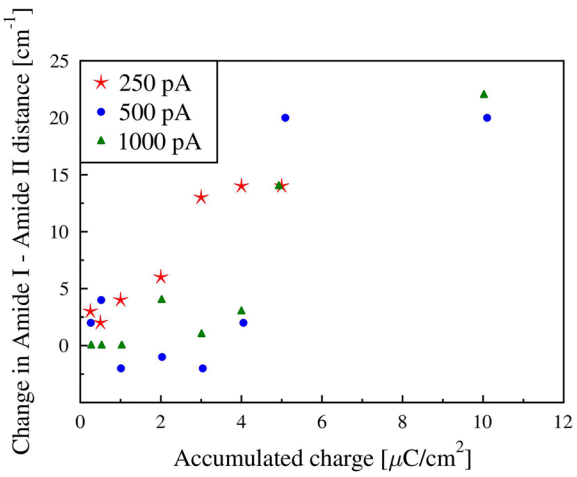

Fig. 3 Changes in the distance of amide I and amide II peaks, compared to the corresponding reference (non-irradiated) area on the same piece of parchment sample

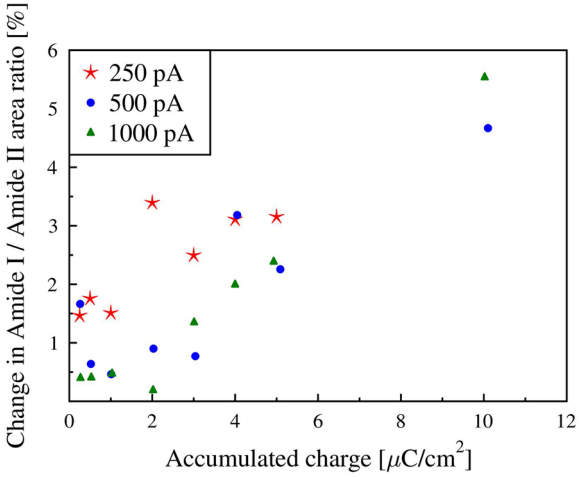

Fig. 4 Changes in the ratio of amide I and amide II peak areas, expressed as percentage of the ratio of the amide I and amide II peak areas for the corresponding reference (non-irradiated) area on the same piece of parchment sample

component. These chemical or structural changes lead to a reduced amount of intermolecular crosslinks [56], and thus can also cause the weakening of the material. We note that Vyskočilová explains the increase of the amide I/amide II peak area ratio observed for acid hydrolysis with the decrease of amide II, not with the increase of amide I, contrary to Derrick. However, acid hydrolysis was not characterized with the shift of the amide II peak [54].

Oxidation of the polypeptide chain can result in the formation of carbonyl compounds, causing the appearance of a shoulder in the 1700–1750 cm^{-1} wavenumber region of the FTIR spectrum. Nevertheless, we could not observe such changes after the proton beam irradiation.

FTIR analysis is an important tool in degradation studies but the information depth is quite small, less than 2 microns in our case. However, the deposited energy of ion beams can be several times bigger in depth of the material than at the surface, so FTIR on the sample surface underestimates the potential harm. Figure 5 shows the deposited energy along the path of the particles calculated with the SRIM programme package [57]. At the beginning of their path, the 2.3 MeV protons lose approx. 16 keV/micron, while before stopping they lose up to 100 keV/micron. When we see some changes on the surface, there is most probably already a damage deep below, similarly to irradiated polymers [58]. In our case, we found definite changes in the FTIR spectra at high doses, such as 5 and 10 $\mu C/cm^2$, but the situation at lower doses was not as univocal. In this study, FTIR was chosen for its non-invasiveness. Nevertheless, FTIR microscopy on cross-sections would be a valuable tool to track changes along the path of protons.

In our case, we can clearly state that reducing the current did not lead to lesser changes observed in the FTIR spectra. Both the shift and relative decrease in amide II could be observed at lower accumulated charges for 250 pA. Indeed, irradiation with lower currents, thus longer in time, may increase the chance for changes mediated by oxygen or intermediary agents, as it was observed in case of certain polymers [59].

Bath test

The H_2O_2 solution was originally used to check the effect of an oxidizing agent on the discoloration caused by the irradiation. However, a gentle stroke with a cotton bud resulted in removing some material from the surface of samples irradiated with higher doses, which was obvious for painted samples (the effect of paint layer is discussed in our previous work [31]). Immersion of the samples in the solution eliminated the additional mechanical interference of stroking. The immersion in liquid resulted in clearly visible marks for higher doses, 2 $\mu C/cm^2$ and upwards, as shown in Fig. 6. Furthermore, addition of H_2O_2 was found to be not necessary, distilled water was sufficient to remove some of the irradiated collagen from the parchment pieces.

Optical coherence tomography

The OCT technique was employed for a limited set of samples (Table 2) to semi-quantitatively examine the modification of the samples caused by the irradiation. This technique could reveal the properties of the "crater" formed in the irradiated parchment samples which suffered the short immersion in water, either with or without H_2O_2.

Samples were scanned with OCT to estimate the width and depth of the "crater" and examine the scattering

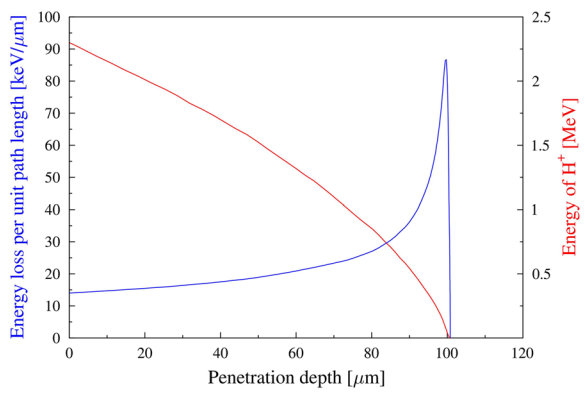

Fig. 5 The Bragg curve: the energy loss of protons per unit distance (blue). The actual energy along the path is represented with the red line

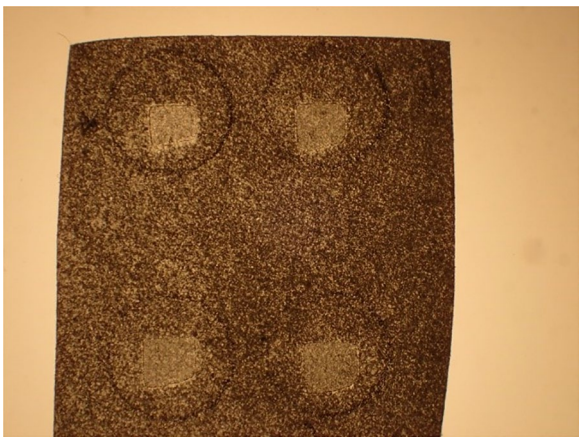

Fig. 6 Transmitted-light photograph of a parchment sample which underwent a short bath [5 min] in 3% H_2O_2 solution. Accumulated charge: 2, 3 (upper left and right spots), 4 and 5 (lower left and right spots) $\mu C/cm^2$, current 1 nA). The photo was taken after drying

Table 2 Results of the OCT examination of the irradiated spots

Sample	Spot	Current (pA)	Charge per unit area (μC/cm^2)	Crater width[a] (μm)	Crater depth[b] (μm)	Treatment (5 min immersion)
T1	1	500	0.5	n. c.[c]	n. c	H_2O
	2		1	2252	~15[d]	
	3		2	1861	97	
	4		3	2362	117	
T2	1	500	0.5	n. c	n. c	3% H_2O_2
	2		1	187	74	
	3		2	2240	76	
	4		3	2502	72	
W1	1	500	0.5	n. c	n. c	No treatment
	2		1	n. c	n. c	
	3		2	n. c	n. c	
	4		3	n. c	n. c	
W4	1	1000	2	2246	80	3% H_2O_2
	2		3	2362	94	
	3		4	2473	80	
	4		5	2619	74	
W6	1	250	2	2392	86	3% H_2O_2
	2		3	2532	86	
	3		4	2642	121	
	4		5	2701	101	

[a] Estimated error = 20 μm

[b] Estimated error = 10 μm

[c] No crater observed

[d] Estimated value, crater almost not detectable

properties of the parchment in the irradiated spot. It is worthwhile to note that in case of samples not subjected to the short immersion in water (W1 in Table 2) neither crater formation nor structure alteration were observed by OCT. In the case of samples treated with water or H_2O_2 solution after being irradiated with 2 μC/cm^2 and upwards, craters were formed with lateral dimension somewhat smaller than the irradiated area, between 1.8 and 2.7 mm, and increasing in size with the applied charge, while the depth varied between 72 and 121 μm (Fig. 7). For higher fluences, the depth of the crater seems to be more related to the penetration depth of protons, which is the same for all fluences, approx. 100 microns. We see craters about this depth. Meanwhile, the width of the crater increases with the deposited charge in all but one instance (T1 spot 1 and 2—but here the depth is informative). These results are in accordance with the SEM cross-section data [31]. Besides the crater formation, a lowered scattering could be observed in the irradiated spot after the short bath in most cases. A lowered scattering indicates more homogeneous, therefore more deteriorated collagen structure.

As for the comparison of the high and low current conditions (1000 pA vs 250 pA, 2–5 μC/cm^2), it must be noticed that the low current (i.e. longer irradiation) resulted in a more pronounced crater formation after the immersion in the hydrogen peroxide solution. This indicates more pronounced changes in the irradiated area, in accordance with the FTIR results.

Low irradiation (at 500 pA), below 2 μC/cm^2 was less harmful to the sample: for 1 μC/cm^2 we only found a small hole (approx. 200 microns wide and 70 microns deep: T2 spot 2 in Table 2; Fig. 8) or a slight indentation (T1 spot 2 in Table 2) after the bath test. Nevertheless, the altered scattering properties could still be observed. The 0.5 μC/cm^2 accumulated charge did not cause observable alterations.

To summarize, the irradiation with 2 μC/cm^2 was too intense for avoiding modifications at all three currents applied, while 1 μC/cm^2 accumulated charge caused some changes, not observable with electron microscopy but revealed by means of the "bath", at 500 pA current. Unfortunately, low current and low charge conditions were not sufficiently and conclusively examined with

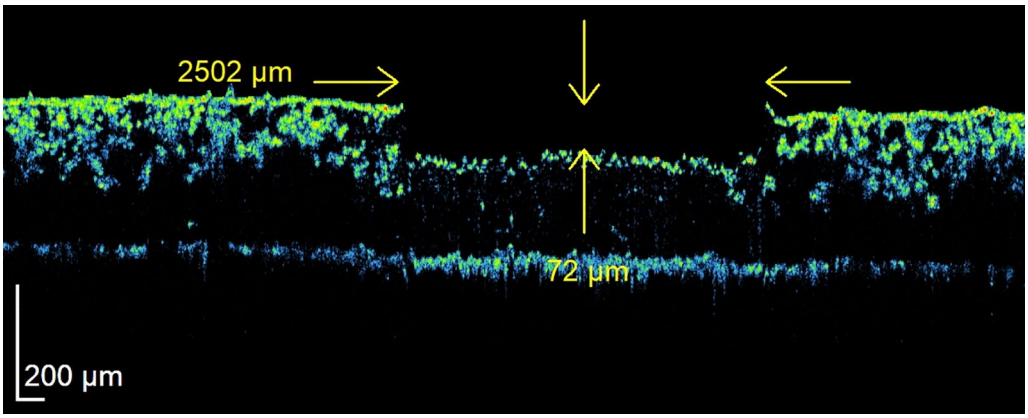

Fig. 7 OCT cross-sectional image of a parchment area subjected to 3 µC/cm^2 proton fluence at 500 pA, and immersed in 3% H_2O_2 solution for 5 min (sample T2, spot 4 in Table 2). The image is strongly expanded in a vertical (in depth) direction and shows a window of 7 mm × 0.70 mm size

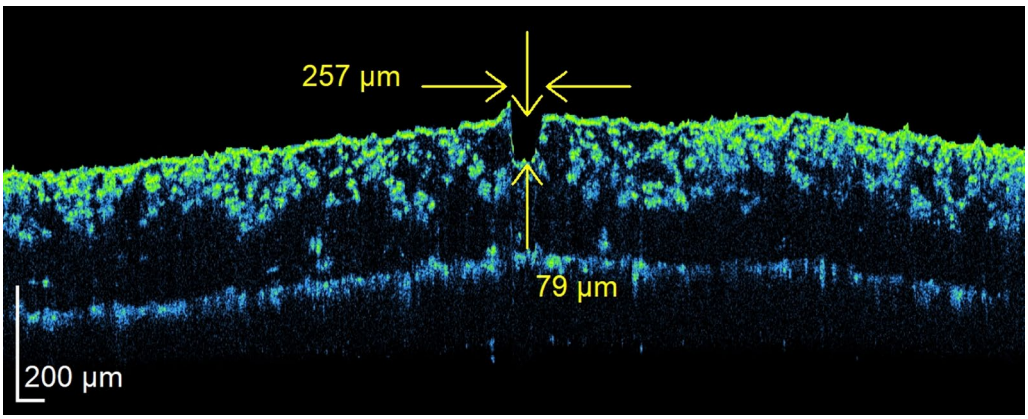

Fig. 8 OCT cross-sectional image of a parchment area subjected to 1 µC/cm^2 proton fluence at 500 pA, and immersed in 3% H_2O_2 solution for 5 min (sample T2, spot 2 in Table 2). The image is strongly expanded in a vertical (in depth) direction and shows a window of 7 mm × 0.70 mm size

OCT. Conditions below 2 µC/cm^2 were investigated only at 500 pA applied current. Therefore, digital 3D microscopy was additionally used for further investigation.

Digital 3D microscopy

Investigation of the low current (250 pA) condition, after a short H_2O_2 bath, showed an altered spot at the 1 µC/cm^2 accumulated charge but no signs of damage were detected at 0.25 or 0.5 µC/cm^2. On the other hand, for the high current (1 nA), i.e., shorter measurement, the 1 µC/cm^2 was found to be harmless, the removability of the irradiated material did not increase. Figure 9 shows the digital 3D image of an area subjected to 10 µC/cm^2 accumulated charge (proton fluence) using 1 nA current. The observed picture is very similar to deliberate micromachining when the material is weakened through radiation and then removed, thus creating a patterned structure.

As for the 1 µC/cm^2 accumulated charge at 250 pA condition, the damaged surface is smaller by 60% and the created crater is much shallower but still observable (Fig. 10.) We note that the two irradiation conditions were applied to two different areas on the same piece of parchment.

Combining OCT and digital 3D microscopy results we can state that, depending on the current, 1 µC/cm^2 might or might not create damage, 2 µC/cm^2 is undoubtedly damaging, and 0.5 µC/cm^2 seems to be safe for the test material used in our study.

Organic objects are not in the main focus of ion beam analysis since this technique is dedicated for elemental analysis of inorganic materials, primarily [60]. However, when quantitative elemental information, depth profile, or information on lighter elements are of interest, IBA might be a good choice [26–29]. A simple "bath test",

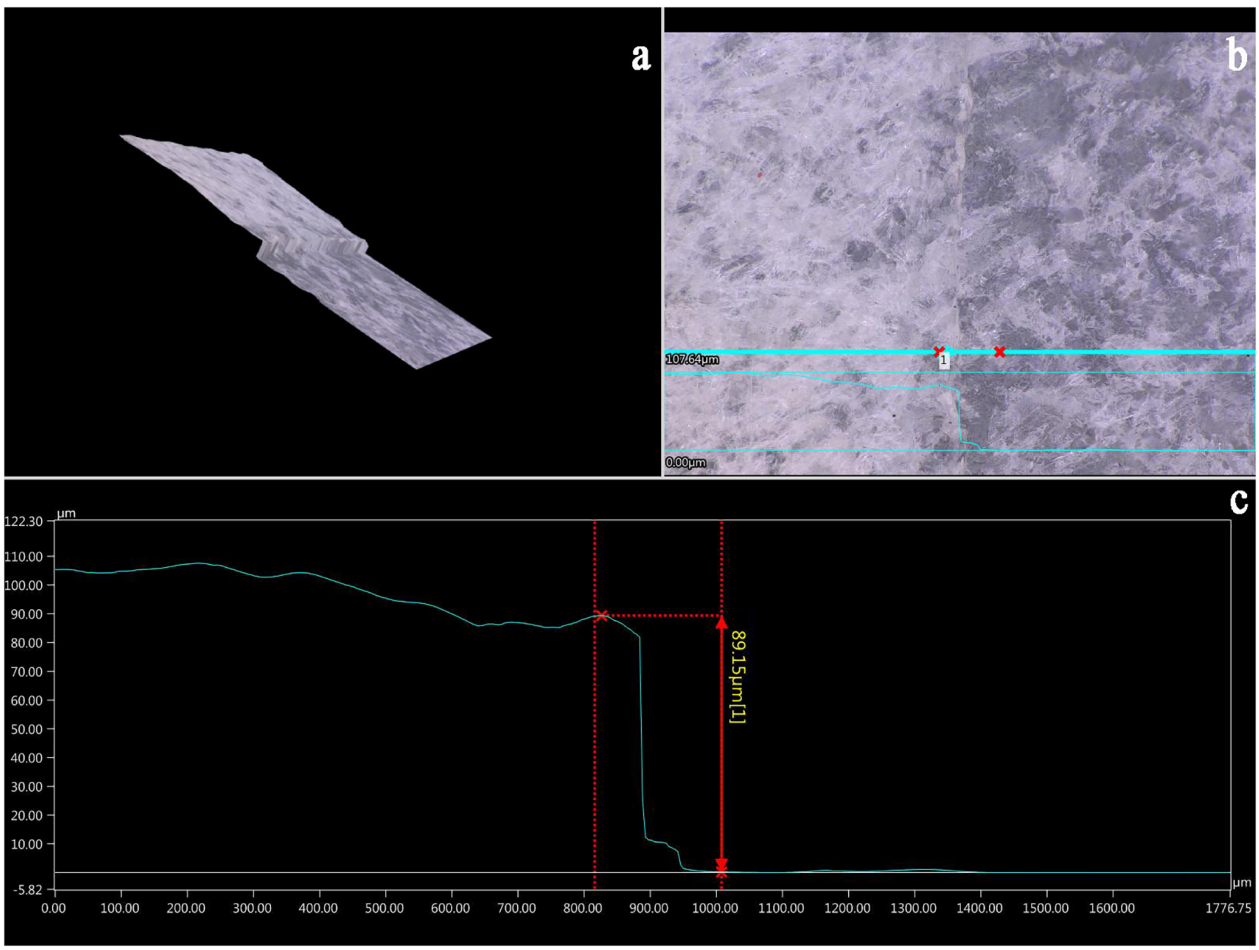

Fig. 9 Digital 3D image (**a**) and depth profile (**b**, **c**) for a parchment area subjected to 10 µC/cm^2 proton fluence at 1 nA, and immersed in 3% H_2O_2 solution for 5 min. The image was taken at the border of the non-irradiated and irradiated areas at one side of the irradiation spot

revealing a small hole, showed that some change was caused already at 1 µC/cm^2, which is not an extraordinarily high dose in ion beam analysis [28]. The changes in the structure of parchment caused the weakening of the material, resulting in increased removability. When the measured objects are relatively large and thick, such as a painting, a tiny hole might not jeopardize the integrity of the object itself. However, for materials such as parchment or paper, with thickness comparable to the penetration depth of ions, it is very important to keep the dose as small as possible or to consider alternative techniques. In this study, we investigated fresh parchment which might be more sensitive than other organic objects. On the other hand, traditionally prepared paper might be even more susceptible to damage. Indeed, Xuan paper was found to be deteriorated at 0.4–0.6 µC/cm^2 [30]. Mechanical properties, water content and hydrothermal stability can change during the ageing of parchment [61–64]. Combining irradiation with artificial ageing [65], either exposing irradiated and non-irradiated samples to artificial ageing and comparing their behaviour or irradiating artificially aged samples to simulate the behaviour of old parchments would be an interesting next step for this research.

Of course, it is not just IBA which might cause harm, Raman spectroscopy or other laser-based techniques and intense X-ray radiation are also able to deposit large amount of energy in a small volume [1, 11, 13, 66]. All of these techniques should only be used for heritage materials when they are safe enough and the information they provide cannot be gathered otherwise.

Conclusions

In this study, we investigated the possible harmful effects of ion beam irradiation on parchment. FTIR results indicate changes in the secondary structure of collagen on the surface of the irradiated parchment samples starting from 2 µC/cm^2 accumulated charge.

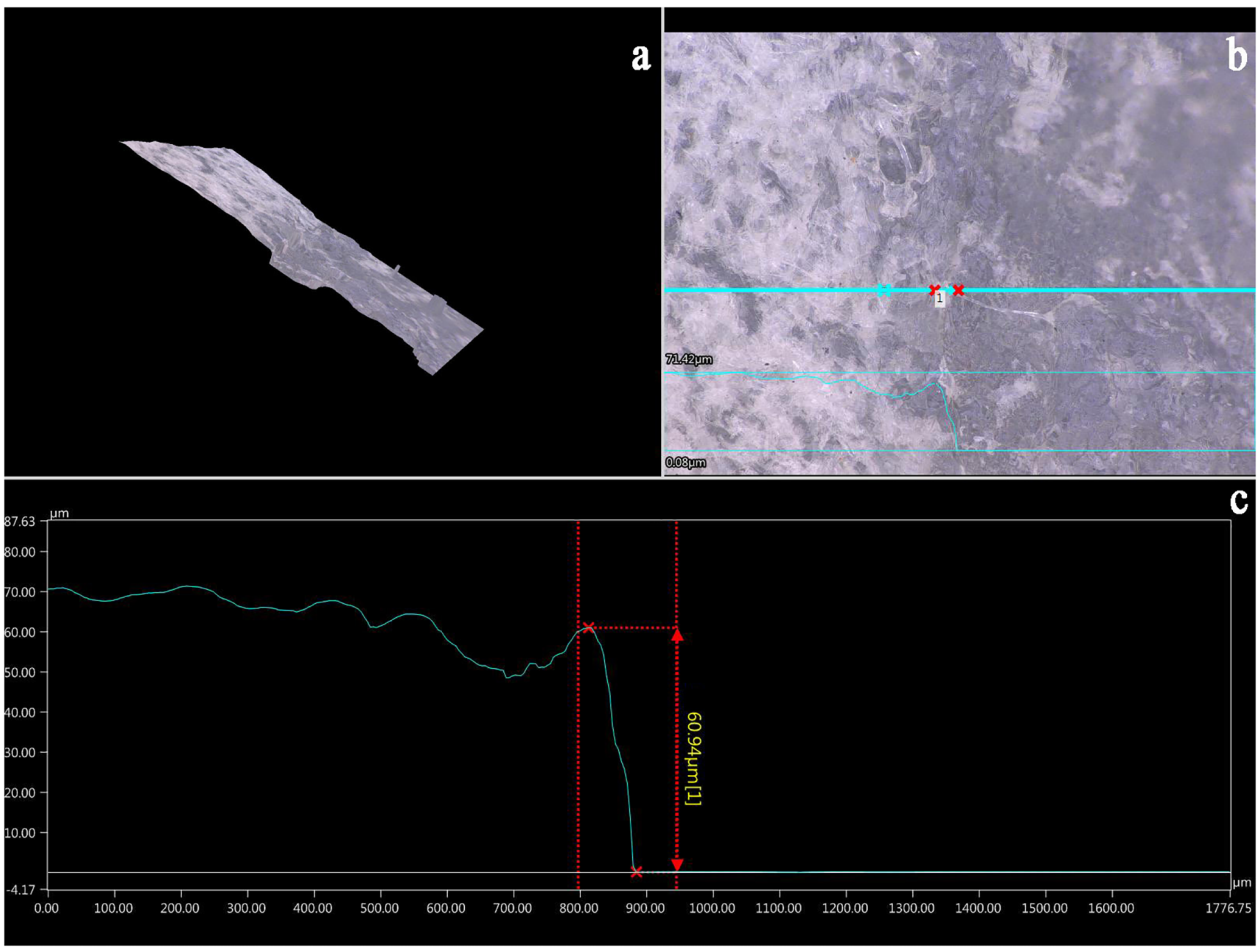

Fig. 10 Digital 3D image (**a**) and depth profile (**b**, **c**) for a parchment area subjected to 1 μC/cm^2 proton fluence at 250 pA, and immersed in 3% H_2O_2 solution for 5 min. The image was taken at the border of the non-irradiated and irradiated areas at one side of the irradiation spot

However, a special feature of ion beam irradiation is that the deposited energy is highest just before stopping in the material, in our case several tens of microns below the surface. Inspection of the surface underestimates the effects and may miss potential damage for which we had an indication using a simple "bath test" (immersion in a 3% H_2O_2 solution) even at 1 μC/cm^2 accumulated charge, depending on the applied current. On the other hand, no such indication emerged for fluences lower than that. However, a relatively low fluence necessitates a detection system of high efficiency to obtain a meaningful analytical signal. Our aim was not to establish absolute safe limits in general or to characterize this specific parchment material exhaustively but to point out that caution must be taken when irradiating sensitive materials with ions for analytical purposes. A refined approach for the further evaluation of the hypothesized modifications in model parchment should be performed using artificial ageing of the samples with controlled parameters in the future, similarly to the study performed on paper material utilizing synchrotron radiation [67].

Abbreviations

ATOMKI: Institute for Nuclear Research, Debrecen, Hungary; FTIR-ATR: Fourier transform infra-red spectroscopy in attenuated total reflectance; IBA: Ion beam analysis; JRA: Joint research activity; OCT: Optical coherence tomography; PIXE: Particle induced X-ray emission; SDD: Silicon drift X-ray detector.

Supplementary Information

The online version contains supplementary material available at https://doi.org/10.1186/s40494-022-00781-8.

Additional file 1: Table S1: Location of amide I and amide II bands and amide I / amide II peak area ratios in the FTIR spectra. Change in distance compared to reference corresponds to Figure 3, relative change in area ratio corresponds to Figure 4 in the main text.

Acknowledgements
The ATOMKI team acknowledges the support of the grant GINOP-2.3.3-15-2016-00029 providing some of the instrumentation. A. A., B. D., Zs. K, Z. Sz. also acknowledge GINOP-2.3.4-15-2020-00007. The NCU team acknowledges use of the infrastructure of Interdisciplinary Centre for Modern Technologies NCU. The samples used in this study come from modern parchment provided by the Handschriftenabteilung of the Staatsbibliothek zu Berlin—Stiftung Preußischer Kulturbesitz. We acknowledge particularly the support of this program by Julia Bispinck-Rossbacher, principal conservator, and Everardus Overgaauw, head of the department.

Author contributions
Conceptualization: ÁCs, ZSz, IR. Sample preparation: KM, IR. Irradiation, FTIR, digital 3D microscopy: ATOMKI team. OCT: PT, MS. All authors participated in the discussion of results. All authors read and approved of the final manuscript.

Funding
Open access funding provided by ELKH Institute for Nuclear Research. Support by the Horizon 2020 Programme of the EU (IPERION CH Grant Agreement no. 654028 and IPERION HS Grant Agreement no. 871034) is gratefully acknowledged.

Availability of data and materials
The datasets used and/or analysed during the current study are available from the corresponding author upon reasonable request.

Declarations

Competing interests
The authors declare that they have no competing interests.

Author details
[1]Institute for Nuclear Research (ATOMKI), Bem tér 18/C, 4026 Debrecen, Hungary. [2]Doctoral School in Physics, University of Debrecen, Egyetem tér 1, 4032 Debrecen, Hungary. [3]Institute of Physics, Faculty of Physics, Astronomy and Informatics, Nicolaus Copernicus University in Toruń, ul. Grudziądzka 5, 87-100 Toruń, Poland. [4]IPANEMA, Ancient Materials Research Platform, USR 3461 CNRS/MC/UVSQ/MNHN, BP48 Saint-Aubin, 91192 Gif-sur-Yvette, France. [5]ENSCP, Institut de Recherche de Chimie Paris, Centre de Recherche et de Restauration des Musées de France, UMR 8247 CNRS/MC, PSL University, 14 Quai François Mitterrand, 75001 Paris, France. [6]New AGLAE, FR 3506 CNRS/MC, C2MRF, 14 Quai François Mitterrand, 75001 Paris, France.

Received: 29 April 2022 Accepted: 23 August 2022
Published online: 07 September 2022

References

1. Carrasco E, Oujja M, Sanz M, Marco JF, Castillejo M. X-ray and ion irradiation effects on azurite, malachite and alizarin pictorial models. Microchem J. 2018;137:381–91.
2. Brunetti B, Miliani C, Rosi F, Doherty B, Monico L, Romani A, et al. Non-invasive investigations of paintings by portable instrumentation: the MOLAB experience. Topics Curr Chem. 2016;374(1).
3. Bertrand L, Schoder S, Anglos D, Breese MBH, Janssens K, Moini M, et al. Mitigation strategies for radiation damage in the analysis of ancient materials. Trac-Trend Anal Chem. 2015;66:128–45.
4. Sendrea C, Carsote C, Radu M, Badea E, Miu L. The effect of gamma irradiation on shrinkage activity of collagen in vegetable tanned leather. Rev Chim-Bucharest. 2017;68(7):1535–8.
5. Patten K, Gonzalez L, Kennedy C, Mills D, Davis G, Wess T. Is there evidence for change to collagen within parchment samples after exposure to an X-ray dose during high contrast X-ray microtomography? a multi technique investigation. Herit Sci. 2013;1(1):22.
6. Kennedy CJ, Vest M, Cooper M, Wess TJ. Laser cleaning of parchment: structural, thermal and biochemical studies into the effect of wavelength and fluence. Appl Surf Sci. 2004;227(1):151–63.
7. Carsote C, Şendrea C, Micu M-C, Adams A, Badea E. Micro-DSC, FTIR-ATR and NMR MOUSE study of the dose-dependent effects of gamma irradiation on vegetable-tanned leather: the influence of leather thermal stability. Radiat Phys Chem. 2021;189: 109712.
8. Ciofini D, Bedeir A, Osticioli I, Elnaggar A, Siano S. Conservation of ethnographic artefacts: selective laser ablation of deposits from doum palm fibers. J Cult Herit. 2017;27:143–52.
9. Ciofini D, Cacciari I, Siano S. Multi-pulse laser irradiation of cadmium yellow paint films: the influence of binding medium and particle aggregates. Measurement. 2018;118:311–9.
10. Mencaglia AA, Osticioli I, Siano S. Development of an efficient and thermally controlled Raman system for fast and safe molecular characterization of paint layers. Measurement. 2018;118:372–8.
11. Osticioli I, Mencaglia AA, Siano S. Temperature-controlled portable Raman spectroscopy of photothermally sensitive pigments. Sens Actuators B Chem. 2017;238:772–8.
12. Osticioli I, Ciofini D, Mencaglia AA, Siano S. Automated characterization of varnishes photo-degradation using portable T-controlled Raman spectroscopy. Spectrochim Acta A. 2017;172:182–8.
13. Dal Fovo A, Sanz M, Mattana S, Oujja M, Marchetti M, Pavone FS, et al. Safe limits for the application of nonlinear optical microscopies to cultural heritage: a new method for in-situ assessment. Microchem J. 2020;154: 104568.
14. Gueriau P, Rueff J-P, Bernard S, Kaddissy JA, Goler S, Sahle CJ, et al. Noninvasive synchrotron-based X-ray Raman scattering discriminates carbonaceous compounds in ancient and historical materials. Anal Chem. 2017;89(20):10819–26.
15. Mackova A, Kucera J, Kamenik J, Havranek V, Smit Z, Giuntini L, et al. Nuclear physics for cultural heritage. Nuovo Cim C-Colloq C. 2019; 42(2–3).
16. Jeynes C. Chapter 10—Ion beam analysis for cultural heritage. In: Adriaens M, Dowsett M, editors. Spectroscopy, diffraction and tomography in art and heritage science. Amsterdam: Elsevier; 2021. p. 335–64.
17. Benzeggouta D, Vickridge I. Handbook on best practice for minimising beam induced damage during IBA. arXiv: Mater Sci. 2013.
18. Larsen R. Microanalysis of parchment: Archetype. 2002.
19. Fessas D, Signorelli M, Schiraldi A, Kennedy CJ, Wess TJ, Hassel B, et al. Thermal analysis on parchments I: DSC and TGA combined approach for heat damage assessment. Thermochim Acta. 2006;447(1):30–5.
20. Mallamace F, Baglioni P, Corsaro C, Chen S-H, Mallamace D, Vasi C, et al. The influence of water on protein properties. J Chem Phys. 2014;141(16):10B616_1.
21. Kennedy CJ, Wess TJ. The structure of collagen within parchment—a review. Restaurator. 2003;24(2):61–80.
22. Bella J. Collagen structure: new tricks from a very old dog. Biochem J. 2016;473(8):1001–25.
23. Cappa F, Paganoni I, Carsote C, Badea E, Schreiner M. Studies on the effects of mixed light-thermal ageing on parchment by vibrational spectroscopy and micro hot table method. Herit Sci. 2020;8(1):15.
24. Badea E, Şendrea C, Carşote C, Adams A, Bluemich B, Iovu H. Unilateral NMR and thermal microscopy studies of vegetable tanned leather exposed to dehydrothermal treatment and light irradiation. Microchem J. 2016;129:158–65.
25. Vilde V, Fourneau M, Charles C, Van Vlaender D, Bouhy J, Poumay Y, et al. Use of polarised light microscopy to improve conservation of parchment. Stud Conserv. 2019;64(5):284–97.
26. Beck L, de Viguerie L, Walter P, Pichon L, Gutiérrez PC, Salomon J, et al. New approaches for investigating paintings by ion beam techniques. Nucl Instrum Methods Phys Res Sect B. 2010;268(11):2086–91.
27. Vodopivec J, Budnar M, Pelicon P. Application of the PIXE method to organic objects. Nucl Instrum Methods Phys Res Sect B. 2005;239(1):85–93.
28. Calligaro T, Gonzalez V, Pichon L. PIXE analysis of historical paintings: is the gain worth the risk? Nucl Instrum Methods Phys Res Sect B. 2015;363:135–43.
29. Budnar M, Simčič J, Rupnik Z, Uršič M, Pelicon P, Kolar J, et al. In-air PIXE set-up for automatic analysis of historical document inks. Nucl Instrum Methods Phys Res Sect B. 2004;219–220:41–7.
30. Zeng XZ, Wu XK, Shao QY, Tang JY, Yang FJ. Radiation-damage in pixe analysis of museum paper-like objects. Nucl Instrum Meth B. 1990;47(2):143–7.

31. Muller K, Szikszai Z, Csepregi A, Huszank R, Kertesz Z, Reiche I. Proton beam irradiation induces invisible modifications under the surface of painted parchment. Sci Rep-Uk. 2022;12(1).
32. Torok Z, Huszank R, Csedreki L, Dani J, Szoboszlai Z, Kertesz Z. Development of a new in-air micro-PIXE set-up with in-vacuum charge measurements in Atomki. Nucl Instrum Meth B. 2015;362:167–71.
33. Campbell JL, Boyd NI, Grassi N, Bonnick P, Maxwell JA. The Guelph PIXE software package IV. Nucl Instrum Meth B. 2010;268(20):3356–63.
34. Drexler W, Fujimoto JG. Optical coherence tomography: technology and applications. Berlin: Springer; 2015.
35. Targowski P, Iwanicka M. Optical coherence tomography: its role in the non-invasive structural examination and conservation of cultural heritage objects—a review. Appl Phys A. 2012;106(2):265–77.
36. Targowski P, Kowalska M, Sylwestrzak M, Iwanicka M. OCT for examination of cultural heritage objects. Optical coherence tomography and its non-medical applications: IntechOpen; 2020; 147.
37. Iwanicka M, Sylwestrzak M, Targowski P. Optical coherence tomography (OCT) for examination of artworks. In: Bastidas DM, Cano E, editors. Advanced characterization techniques, diagnostic tools and evaluation methods in heritage science. Cham: Springer International Publishing; 2018. p. 49–59.
38. Callewaert T, Guo J, Harteveld G, Vandivere A, Eisemann E, Dik J, et al. Multi-scale optical coherence tomography imaging and visualization of Vermeer's Girl with a Pearl Earring. Opt Express. 2020;28(18):26239–56.
39. Almasian M, Tiennot M, Fiske LD, Hermens E. The use of ground glass in red glazes: structural 3D imaging and mechanical behaviour using optical coherence tomography and nanoindentation. Herit Sci. 2021;9(1):66.
40. Moretti P, Iwanicka M, Melessanaki K, Dimitroulaki E, Kokkinaki O, Daugherty M, et al. Laser cleaning of paintings: in situ optimization of operative parameters through non-invasive assessment by optical coherence tomography (OCT), reflection FT-IR spectroscopy and laser induced fluorescence spectroscopy (LIF). Herit Sci. 2019;7(1):44.
41. Góra M, Pircher M, Götzinger E, Bajraszewski T, Strlic M, Kolar J, et al. Optical coherence tomography for examination of parchment degradation. Laser Chem. 2006;2006: 068679.
42. Targowski P, Pronobis-Gajdzis M, Surmak A, Iwanicka M, Kaszewska EA, Sylwestrzak M. The application of macro-X-ray fluorescence and optical coherence tomography for examination of parchment manuscripts. Stud Conserv. 2015;60(sup1):S167–77.
43. Pichon L, Moignard B, Lemasson Q, Pacheco C, Walter P. Development of a multi-detector and a systematic imaging system on the AGLAE external beam. Nucl Instrum Meth B. 2014;318:27–31.
44. Clough RL, Gillen KT, Malone GM, Wallace JS. Color formation in irradiated polymers. Radiat Phys Chem. 1996;48(5):583–94.
45. Barth A. Infrared spectroscopy of proteins. Biochim Biophys Acta (BBA) Bioenerget. 2007;1767(9):1073–101.
46. De Meutter J, Goormaghtigh E. FTIR imaging of protein microarrays for high throughput secondary structure determination. Anal Chem. 2021;93(8):3733–41.
47. Sendrea C, Carsote C, Badea E, Adams A, Niculescu M, Iovu H. Non-invasive characterisation of collagen-based materials by NMR-mouse and ATR-FTIR. Sci Bull B Chem Mater Sci UPB. 2016;78:27–38.
48. Boyatzis SC, Velivasaki G, Malea E. A study of the deterioration of aged parchment marked with laboratory iron gall inks using FTIR-ATR spectroscopy and micro hot table. Herit Sci. 2016;4(1):13.
49. Derrick M. Evaluation of the state of degradation of dead sea scroll samples using FT-IR spectroscopy. The Book and Paper Group Annual. 1991;10.
50. Gonzalez L, Wess T. Use of attenuated total reflection-Fourier transform infrared spectroscopy to measure collagen degradation in historical parchments. Appl Spectrosc. 2008;62(10):1108–14.
51. Warren JRS, Tillman WJ. Internal reflectance spectroscopy and the determination of the degree of denaturation of insoluble collagen. J Am Leather Chem Assoc. 1969;1:4–11.
52. Boryskina OP, Bolbukh TV, Semenov MA, Gasan AI, Maleev VY. Energies of peptide–peptide and peptide–water hydrogen bonds in collagen: evidences from infrared spectroscopy, quartz piezogravimetry and differential scanning calorimetry. J Mol Struct. 2007;827(1):1–10.
53. Barth A, Zscherp C. What vibrations tell about proteins. Q Rev Biophys. 2003;35(4):369–430.
54. Vyskočilová G, Ebersbach M, Kopecká R, Prokeš L, Příhoda J. Model study of the leather degradation by oxidation and hydrolysis. Herit Sci. 2019;7(1):26.
55. Kudo S, Ogawa H, Yamakita E, Watanabe S, Suzuki T, Nakashima S. Adsorption of water to collagen as studied using infrared (IR) microspectroscopy combined with relative humidity control system and quartz crystal microbalance. Appl Spectrosc. 2017;71(7):1621–32.
56. Riaz T, Zeeshan R, Zarif F, Ilyas K, Muhammad N, Safi SZ, et al. FTIR analysis of natural and synthetic collagen. Appl Spectrosc Rev. 2018;53(9):703–46.
57. Ziegler JF, Ziegler MD, Biersack JP. SRIM—the stopping and range of ions in matter (2010). Nucl Instrum Methods Phys Res Sect B. 2010;268(11):1818–23.
58. Szilasi SZ, Huszank R, Szikra D, Váczi T, Rajta I, Nagy I. Chemical changes in PMMA as a function of depth due to proton beam irradiation. Mater Chem Phys. 2011;130(1):702–7.
59. Bartczak WM. Relaxation processes connected with electron localization—a review of recent theoretical research in institute of applied radiation-chemistry. Radiat Phys Chem. 1981;17(6):465–80.
60. Zucchiatti A. Ion beam analysis for the study of our cultural heritage. A short history and its milestones. Nucl Inst Methods Phys Res B. 2019;452:48–54.
61. Cappa F, Paganoni I, Carsote C, Schreiner M, Badea E. Studies on the effect of dry-heat ageing on parchment deterioration by vibrational spectroscopy and micro hot table method. Polym Degrad Stab. 2020;182: 109375.
62. Carşote C, Budrugeac P, Decheva R, Haralampiev NS, Miu L, Badea E. Characterization of a byzantine manuscript by infrared spectroscopy and thermal analysis. Rev Roum Chim. 2014;59(6–7):429–36.
63. Gonzalez L, Wade M, Bell N, Thomas K, Wess T. Using attenuated total reflection fourier transform infrared spectroscopy (ATR FT-IR) to study the molecular conformation of parchment artifacts in different macroscopic states. Appl Spectrosc. 2013;67(2):158–62.
64. Odlyha M, Theodorakopoulos C, de Groot J, Bozec L, Horton M. Fourier transform infra-red spectroscopy (ATR/FTIR) and scanning probe microscopy of parchment. e-Preserv Sci. 2009;6:138–44.
65. Milota P, Reiche I, Duval A, Forstner O, Guicharnaud H, Kutschera W, et al. PIXE measurements of Renaissance silverpoint drawings at VERA. Nucl Instrum Methods Phys Res Sect B. 2008;266(10):2279–85.
66. Gervais C, Thoury M, Reguer S, Gueriau P, Mass J. Radiation damages during synchrotron X-ray micro-analyses of Prussian blue and zinc white historic paintings: detection, mitigation and integration. Appl Phys Mater. 2015;121(3):949–55.
67. Gimat A, Schöder S, Thoury M, Dupont A-L. Degradation of historical paper induced by synchrotron X-ray technical examination. Cellulose. 2022;29(8):4347–64.

Publisher's Note